

Lab 5: Digital Image Correlation

Kevin Nguyen

1629535

kln97@uw.edu

Section AC

Revision by Zachary Taylor

Abstract

Digital Image Correlation (DIC) is an innovative non-contact optical technique for measuring strain and displacement. This experiment involves the application of uniaxial tension to EPDM rubber specimens with and without a hole in order to determine the accuracy of digital image correlation and the theoretical model by comparing the theoretical and experimental values of the strain at 3% and 9% applied strain. The average percent error of maximum strain at 3% applied strain is 44.637%. The average percent error of maximum strain at 9% applied strain is 50.71%. The average percent error of minimum strain at 3% applied strain is 163.99%. The average percent error of minimum strain at 9% applied strain is 165.75%. Our findings show that the theoretical model is more accurate at smaller applied strains, with some discrepancy in these findings due to noise in the DIC. In addition, we learned qualitatively that the DIC plots matched those of the theoretical plots relatively well, minus a few differences due to noise. Ultimately, digital image correlation is a useful tool for understanding the strain state of a material under a certain load, but it must be noted that the technique is prone to noise, and its precision heavily depends on things such as speckle pattern, subset size, and camera resolution. The theoretical model is a useful tool for predicting the strain state of a holed specimen, but the model will work best under a small applied strain with as close as possible to a semi-infinite plate.

1. Introduction

Digital Image Correlation (DIC) is an innovative non-contact optical technique for measuring strain and displacement [1]. DIC works by comparing digital photographs of a component at different stages of deformation. By tracking subsets of pixels, the system can measure surface displacement and build up full field 2D or 3D deformation vector fields and strain contour plots. DIC has several advantages over conventional non-destructive methods and some of the other optical techniques such as laser shearography and speckle interferometry, which are generally costlier and more difficult to use outside the laboratory as they require precise setup and low vibrational environments. Also, the equipment is not always suitable for use outdoors. In

contrast, DIC in combination with civil engineering surveying techniques can be used to provide suitably accurate measurements of structures in typical outdoor environments. Any changes in the structure can easily be compared to the captured images, so abnormalities that might be caused by unexpected changes, like a bird landing on a bridge, can be easily identified. Some examples of projects that have been explored using DIC include measuring thermal expansion and distortion of electronic components, measuring the mechanical properties of nuclear graphite, 3D shape measurement on air bags, and strain development during the processing of chocolate. The objective of this laboratory experiment is to compare the stress-strain state of two EPDM rubber specimens under a tensile load, one with and without a hole [2]. In addition, the experimental strains obtained by DIC will be compared to theoretical values in order to explore sources of error present in DIC.

2. Procedure

In this experiment, we obtained two EPDM rubber samples with dimensions 131mm x 25mm x 2.05mm, one of which contains a 4.35mm diameter hole and tested them under a tensile load using an Instron 5586 machine fitted with a load cell. The rubber samples are marked with a speckle pattern from white aerosol spray paint in order to properly analyze them using DIC. To obtain a good speckle pattern, the specimens are laid on the ground and sprayed horizontally across the surface instead of spraying directly at the sample. The difference between a good and bad speckle pattern is shown in Figure 1.

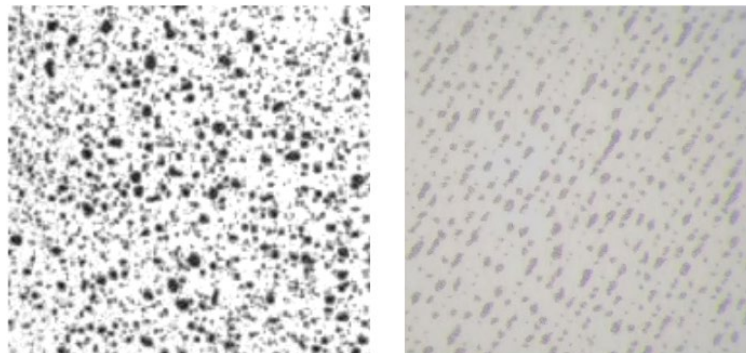


Figure 1: *Good (left) vs. bad (right) speckle pattern*

No special lighting was utilized, laboratory lighting that was diffuse and originated from more than one source was sufficient. The camera exposure is set such that it is low enough for all speckles to be visible, but still create high contrast between the specimen and the speckles. Force data is recorded with the load cell, and displacement data is measured with a linear variable displacement transducer. One camera is set up to record a 2D displacement video. Data is analyzed using a built-in DIC analysis application for the Instron 5586. An image of the test set up is shown in Figure 2.

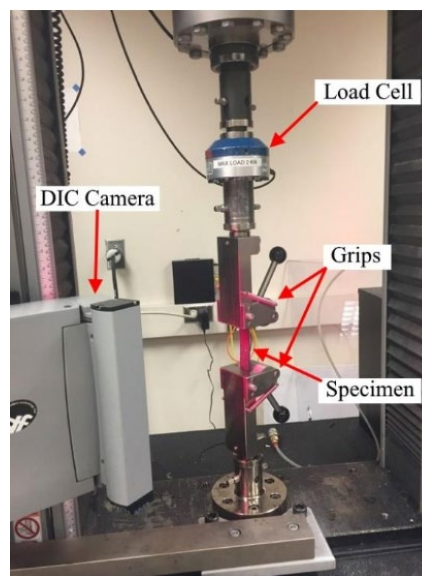


Figure 2: Test setup for DIC lab

3. Results

3.1 – Tension of a Plate with a Hole

For the uniaxial tension of a semi-infinite plate, there will be a uniform stress parallel to the direction of loading. When a circular hole is added to the center of the plate, the stress distribution changes to account for the flaw in the material. Far from the hole, the stress is approximately equal to the applied stress, but near the hole, there an increased stress

concentration. This increased stress concentration at the hole is defined by the following equations:

$$\sigma_{rr} = \frac{\sigma_{\infty}}{2} \left(\left(1 - \left(\frac{a}{r} \right)^2 \right) + \cos(2\theta) \left(3 \left(\frac{a}{r} \right)^4 - 4 \left(\frac{a}{r} \right)^2 + 1 \right) \right) , \quad (3.10)$$

$$\sigma_{\theta\theta} = \frac{\sigma_{\infty}}{2} \left(\left(1 + \left(\frac{a}{r} \right)^2 \right) - \cos(2\theta) \left(3 \left(\frac{a}{r} \right)^4 + 1 \right) \right) , \quad (3.11)$$

$$\sigma_{r\theta} = \frac{\sigma_{\infty} \sin(2\theta)}{2} \left(3 \left(\frac{a}{r} \right)^4 - 2 \left(\frac{a}{r} \right)^2 - 1 \right) , \quad (1.12)$$

Where σ_{∞} is the far field stress, a is the hole radius and r is the distance from the center of the hole. These equations can be derived using the Airy stress function.

Along the edge of the hole, the maximum hoop stress is equal to 3σ , which is a tensile stress that occurs parallel to the loading at $\theta = \pm 90^\circ$. The minimum hoop stress is equal to $-\sigma$, which is a compressive stress that occurs perpendicular to the applied stress at $\theta = 0^\circ$ and $\theta = 180^\circ$. These maximum and minimum stresses are illustrated in Figure 3.

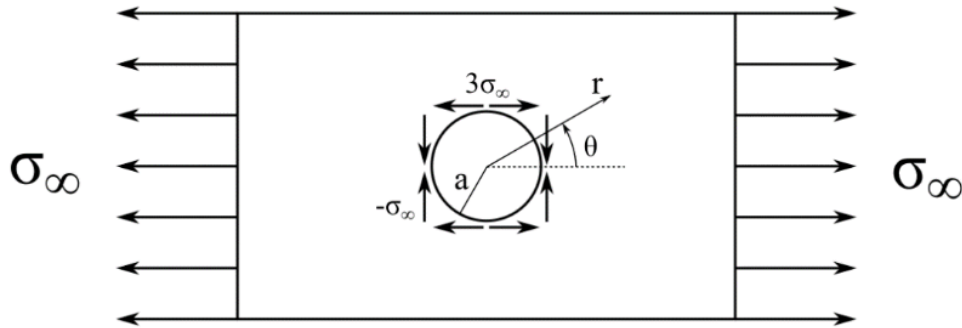


Figure 3: Thin plate with a hole with an applied uniaxial tension

For the purposes of being able to more easily understand our stresses and strains, the following transformation equations from polar to Cartesian coordinates will be used:

$$\sigma_{xx} = \sigma_{rr} \cos^2 \theta + \sigma_{\theta\theta} \sin^2 \theta - \sigma_{r\theta} \sin 2\theta \quad (3.13)$$

$$\sigma_{yy} = \sigma_{rr} \sin^2 \theta + \sigma_{\theta\theta} \cos^2 \theta + \sigma_{r\theta} \sin 2\theta \quad (3.14)$$

$$\sigma_{xy} = \sin \theta \cos \theta (\sigma_{rr} - \sigma_{\theta\theta}) + \sigma_{r\theta} \cos 2\theta \quad (3.15)$$

In order to convert these stresses into strains, 3D Hooke's Law can be utilized. However, since we have a 2D stress, our equations will simplify to the following:

$$\varepsilon_{xx} = \frac{1}{E} (\sigma_{xx} - \nu \sigma_{yy}) \quad (3.16)$$

$$\varepsilon_{yy} = \frac{1}{E} (\sigma_{yy} - \nu \sigma_{xx}) \quad (3.17)$$

$$\gamma_{xy} = \frac{\sigma_{xy}}{G} \quad (3.18)$$

3.2 – Stress vs. Strain Response

In section 3.1, it was noted that for the uniaxial tension of a semi-infinite plate, there will be a uniform stress parallel to the direction of loading. When a circular hole is added to the center of the plate, the stress distribution around the hole changes to account for the flaw in the material. However, far from the hole, the stress should remain relatively the same. As shown in Figure 4, this notion appears to hold true.

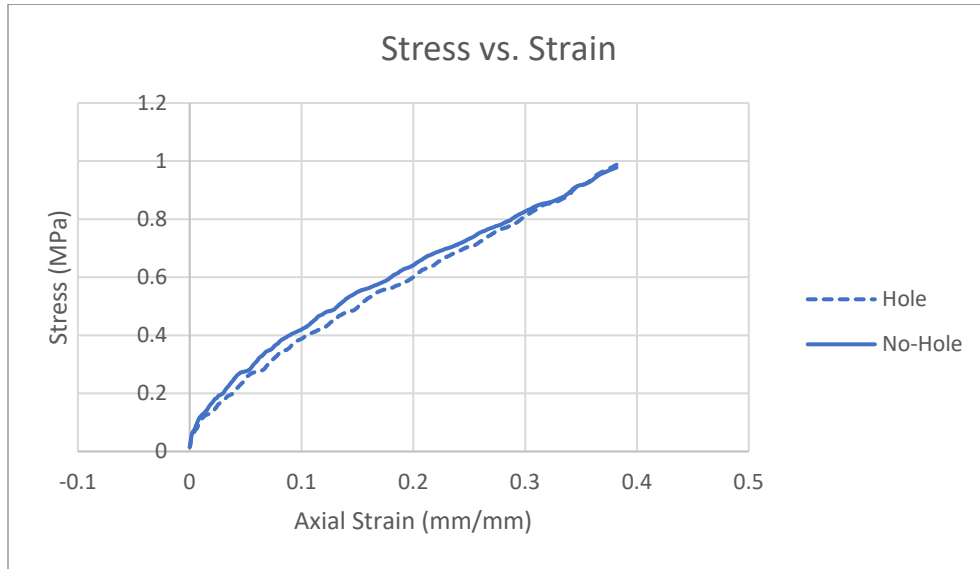


Figure 4: Stress vs. strain plot for EPDM rubber specimen with vs. without a hole

3.3 – DIC Contour Plots

Contour plots are generated for a “small” strain of 3%, and a finite strain of 9% using video footage from the DIC camera. In order to determine the timeframe in the video footage for our desired strain, the following equation was used:

$$\text{Applied \% strain} * L = \Delta L \quad (3.30)$$

where ΔL is extension, and L is the original length of the material. For the rubber specimens with $L = 131\text{mm}$, the extensions are 3.93mm and 11.79mm for the 3% and 9% strain respectively. By pausing the video when the original length of the specimen has elongated by an amount ΔL , we can capture an image of the contour plot at that particular strain. This is particularly easy to accomplish utilizing a sticky note placed at the top of a specimen in the video with a marking of length ΔL . Contour plots for the hole and no hole specimen are paired together by strain amount and strain type (axial, transverse, shear).

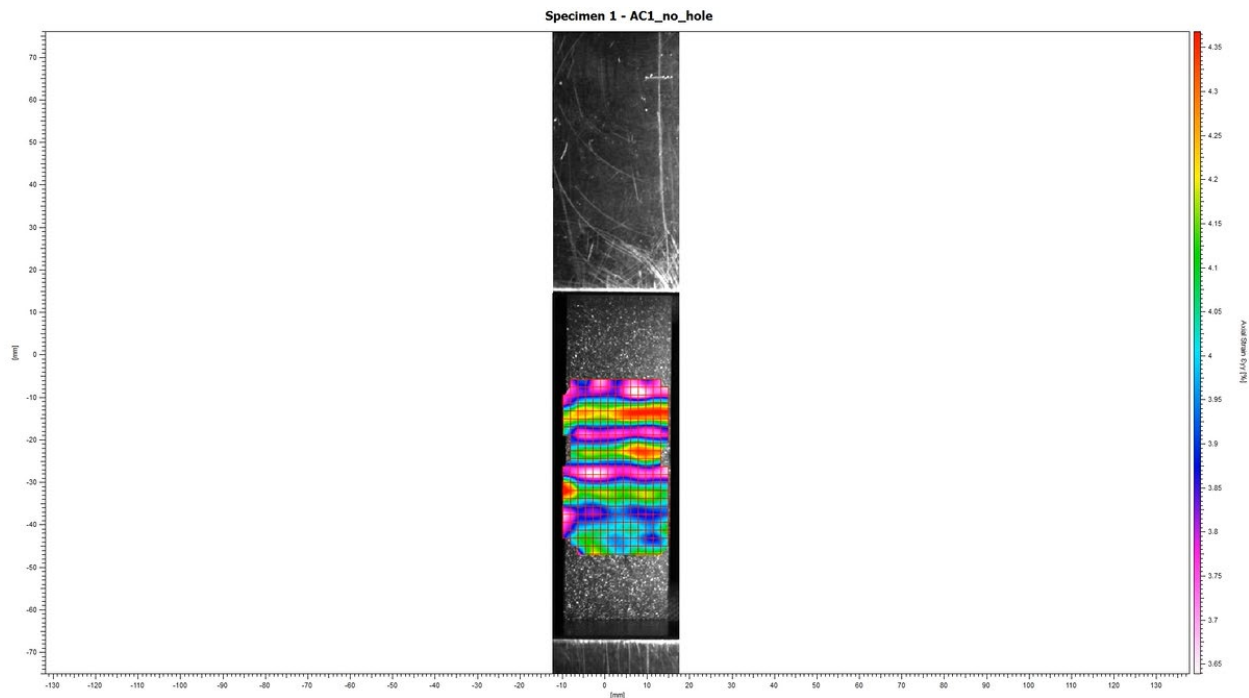


Figure 5: Axial strain at 3% applied strain, no hole.

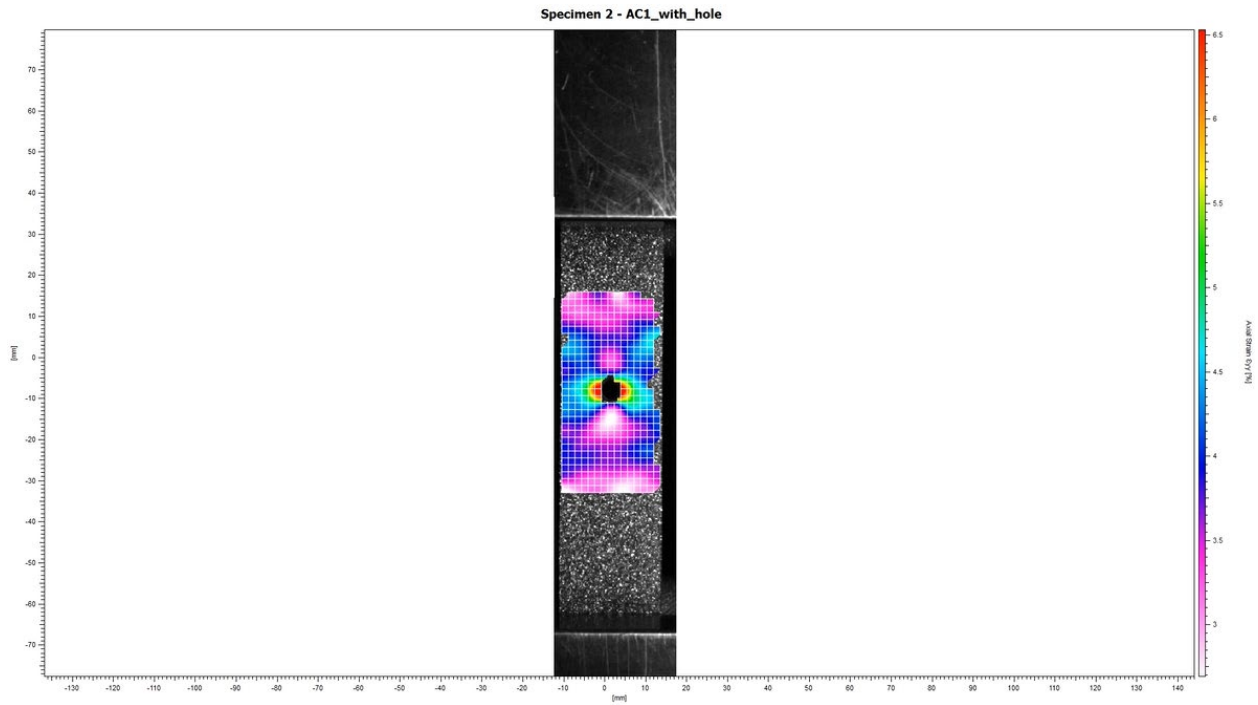


Figure 6: Axial strain at 3% applied strain, with hole.

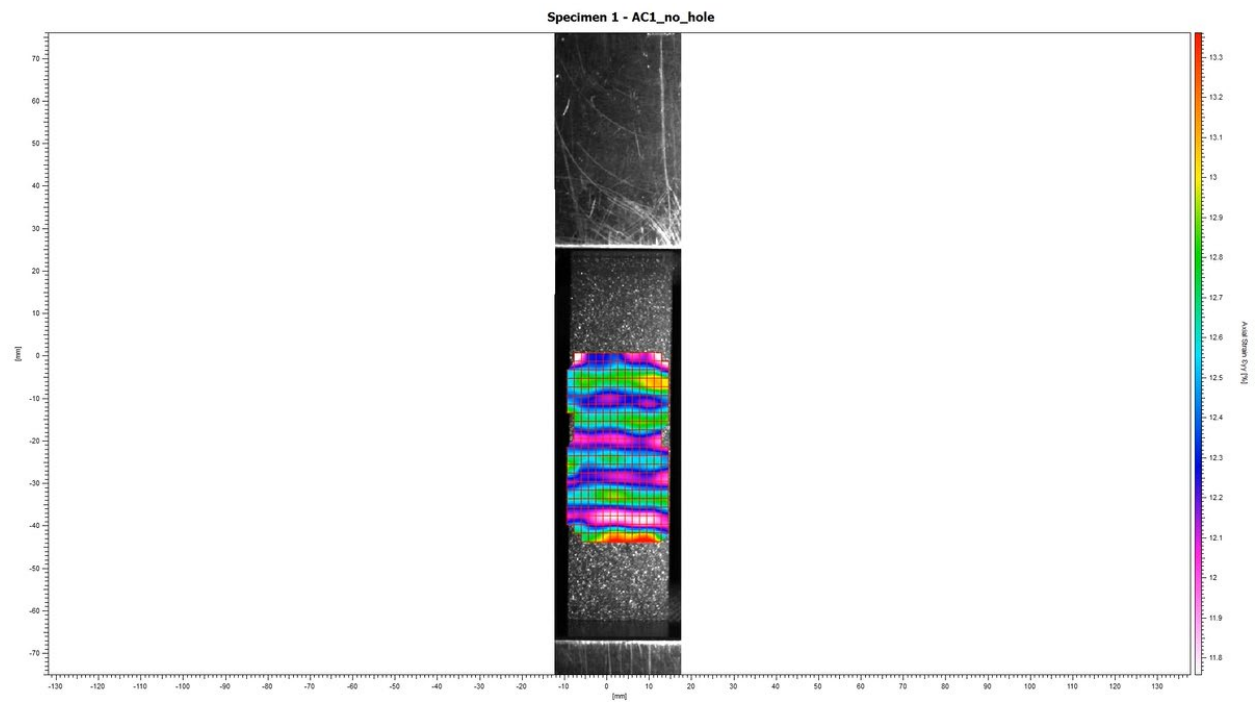


Figure 7: Axial strain at 9% applied strain, no hole.

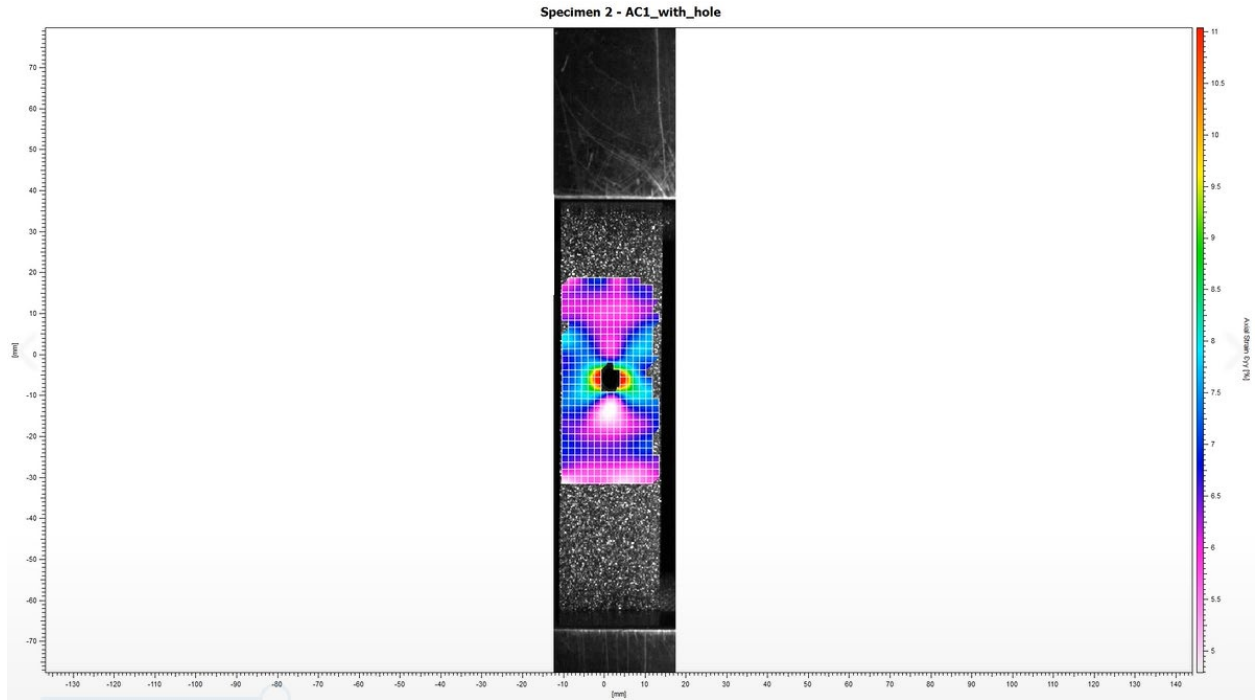


Figure 8: Axial strain at 9% applied strain, with hole.

Figures 4-8 depict axial strains ϵ_{xx} , which can be determined via equation 3.16.

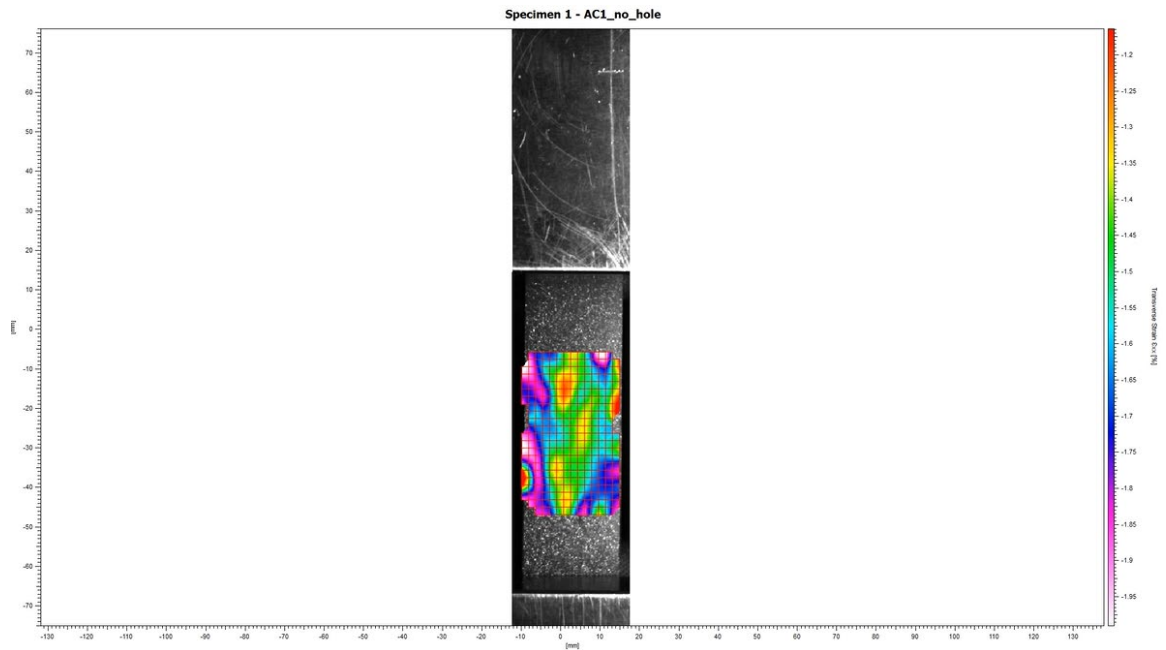


Figure 9: Transverse strain at 3% applied strain, no hole.

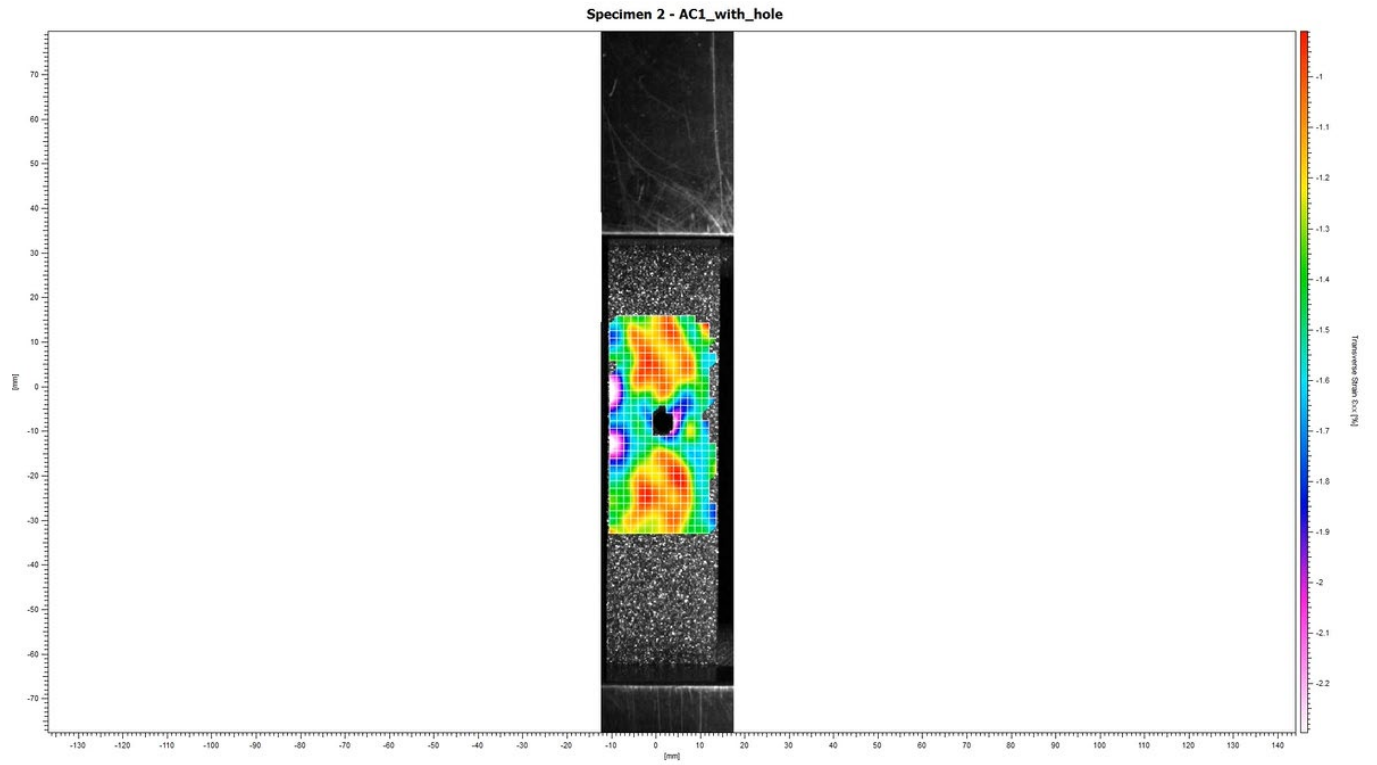


Figure 10: Transverse strain at 3% applied strain, with hole.

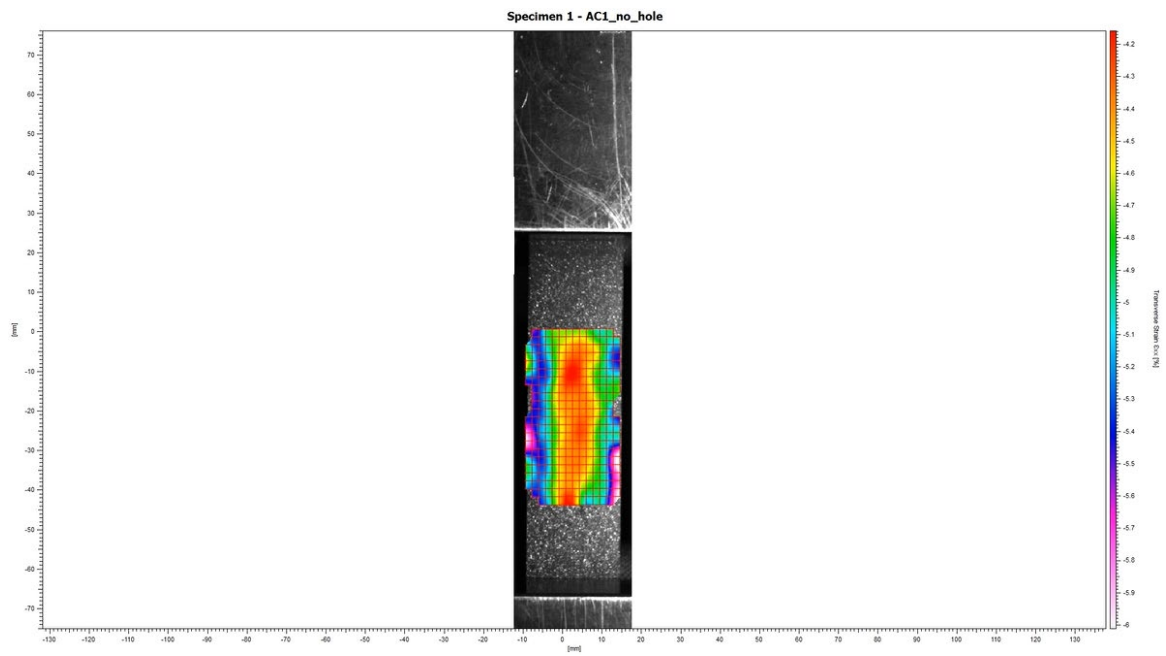


Figure 11: Transverse strain at 9% applied strain, no hole.

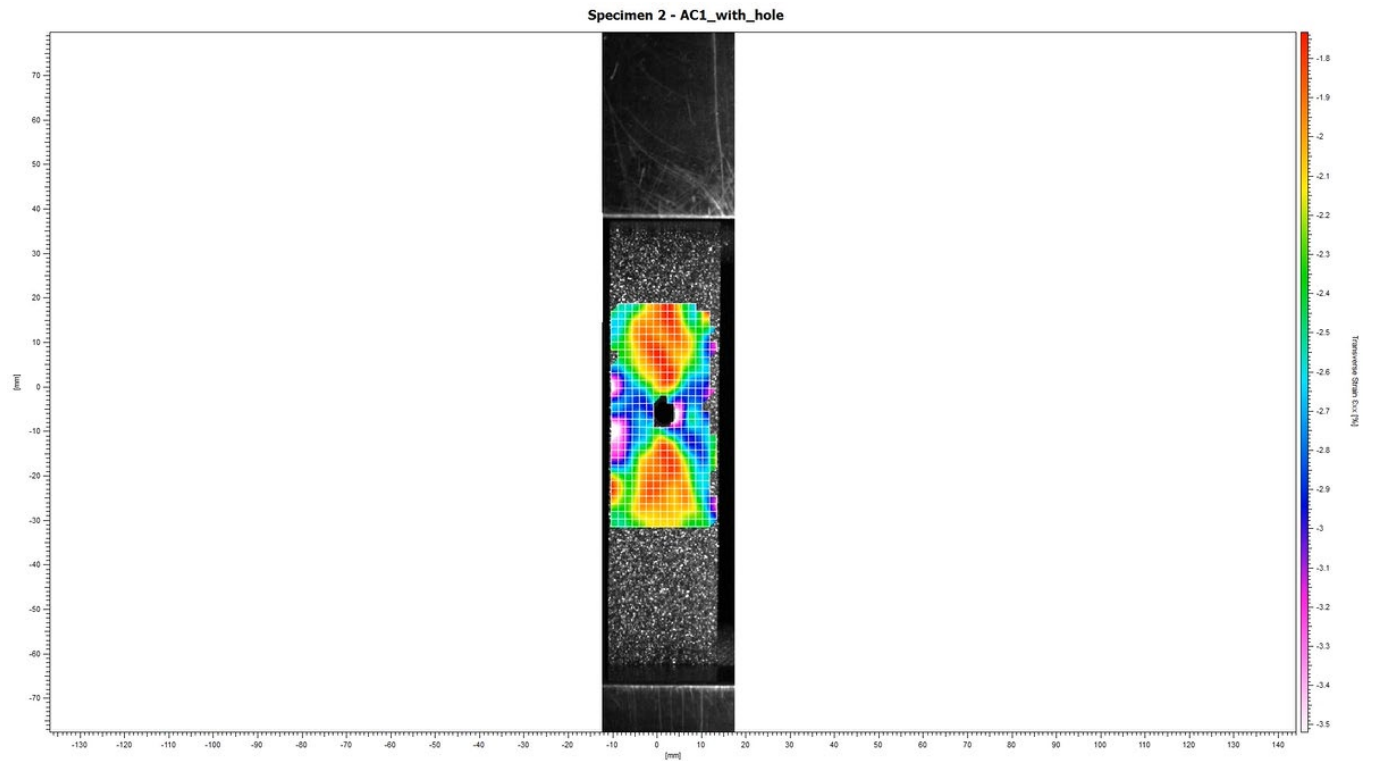


Figure 12: Transverse strain at 9% applied strain, with hole.

Figures 9-12 depict transverse strains ϵ_{yy} , which can be determined via equation 3.17.

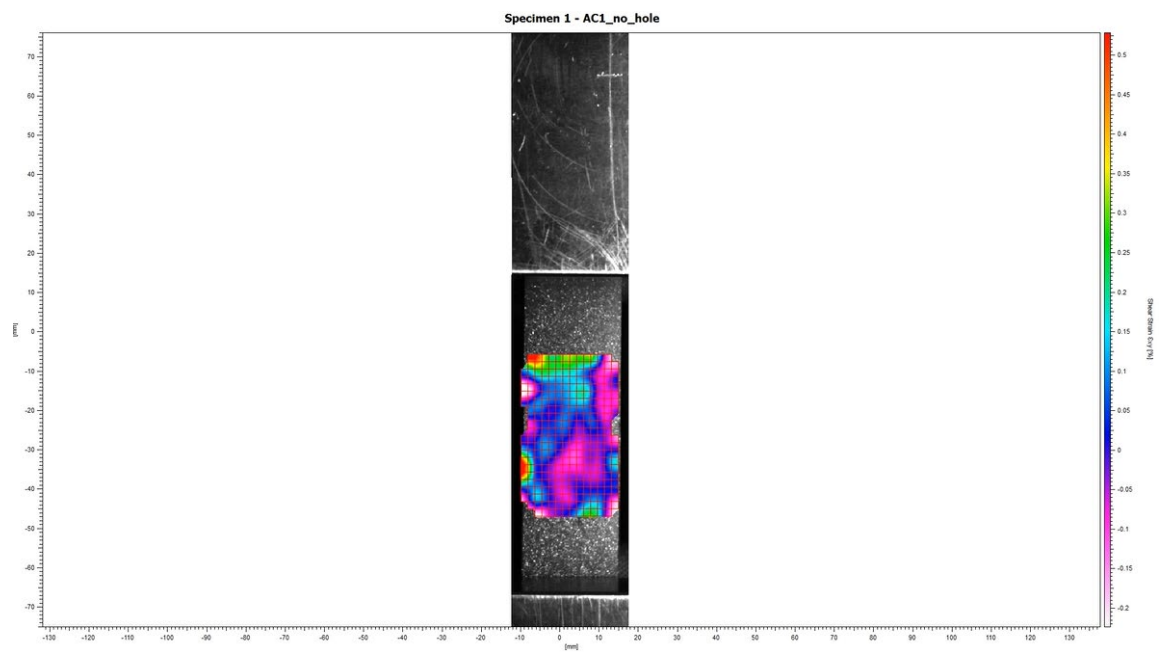


Figure 13: Shear strain at 3% applied strain, no hole.

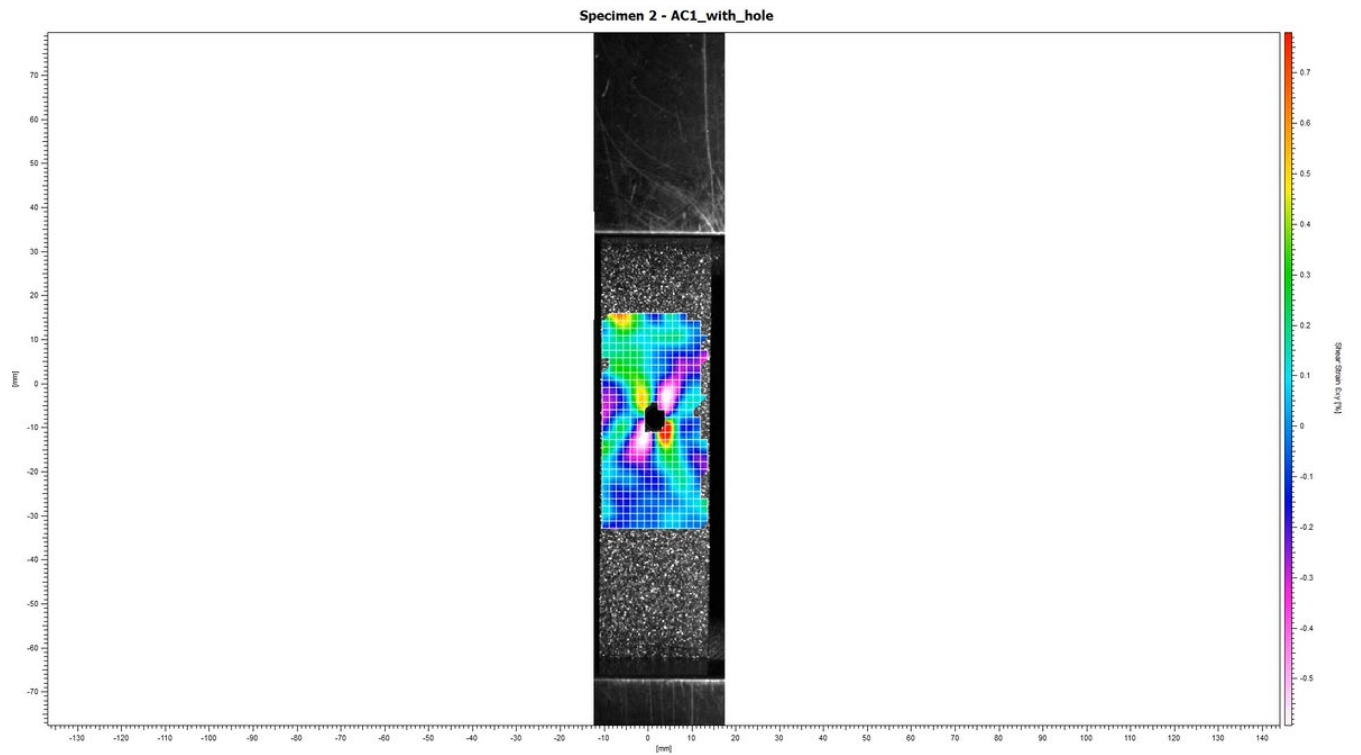


Figure 14: Shear strain at 3% applied strain, with hole.

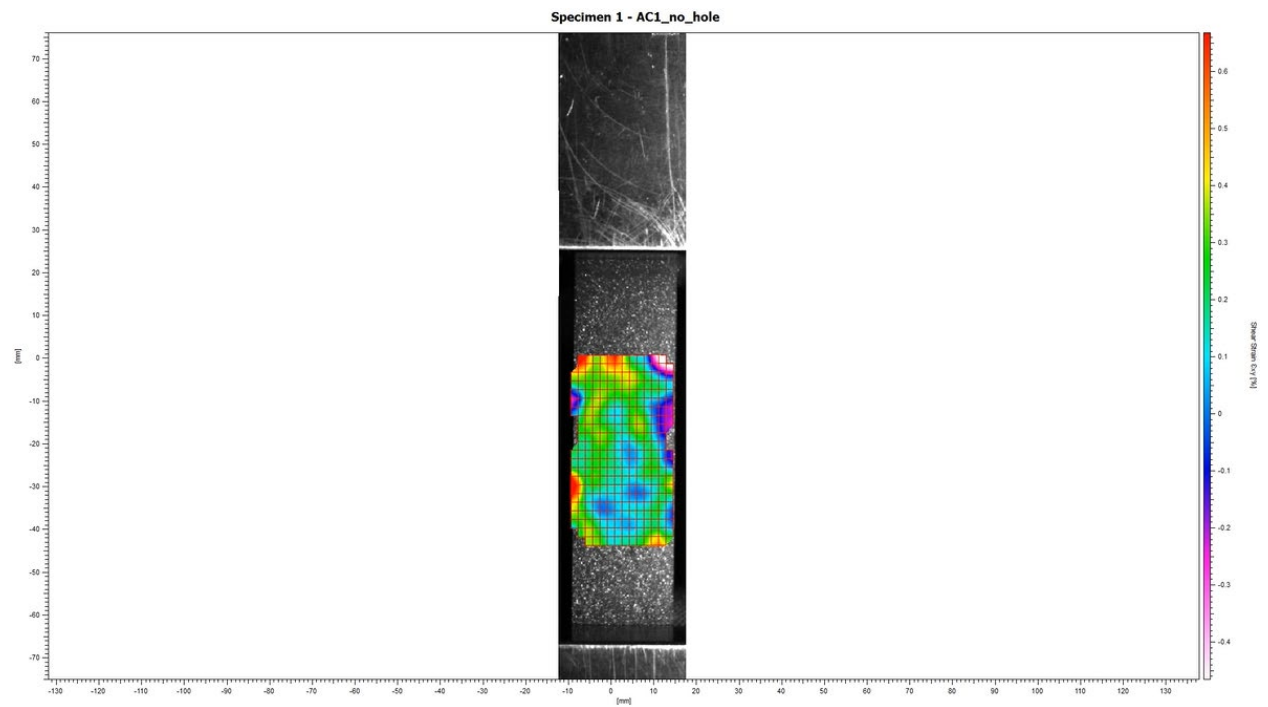


Figure 15: Shear strain at 9% applied strain, no hole.

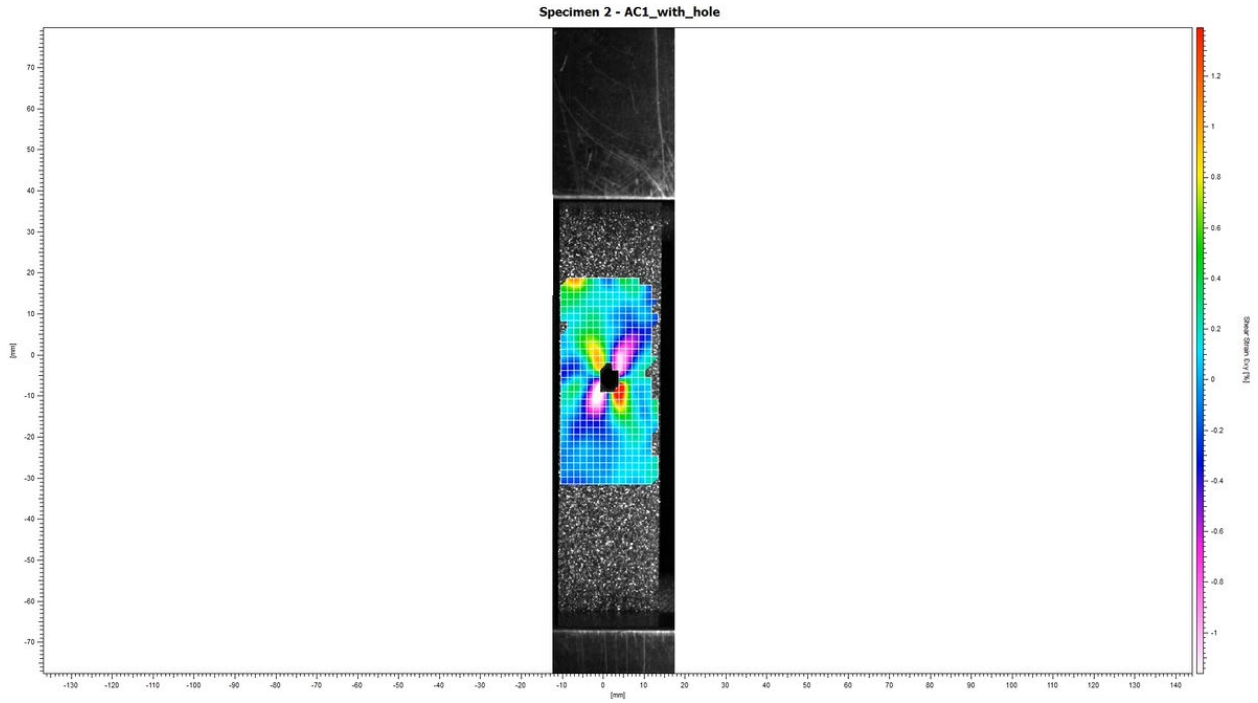


Figure 16: *Shear strain at 9% applied strain, with hole.*

Figures 9-12 depict shear strains ε_{xy} , which can be determined via equation 3.18.

3.4 – Theoretical Contour Plots

Theoretical contour plots are generated for a “small” strain of 3%, and a finite strain of 9% for the specimen with a hole via Matlab. Strains are derived from equations 3.10-3.18 written as Matlab code. By inputting dimensions such as height and width and hole diameter of the specimen, in addition to other parameters like Young’s Modulus, Poisson’s ratio and the applied stress, Matlab has enough information to generate the strain field for a given specimen. In terms of the equations themselves, since we have input an applied stress and hole diameter, Matlab simply calculates the stress/strain response for any given r distance away from the hole.

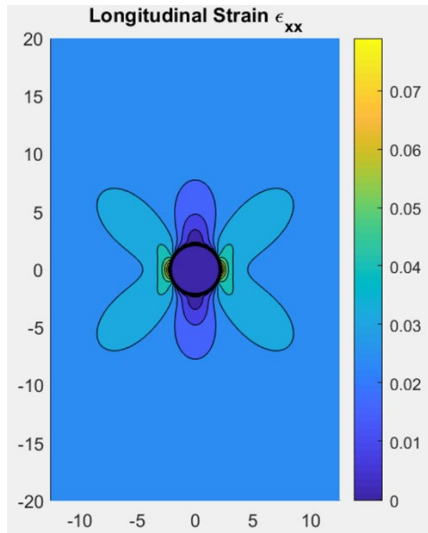


Figure 17: Axial strain at 3% applied strain, with hole

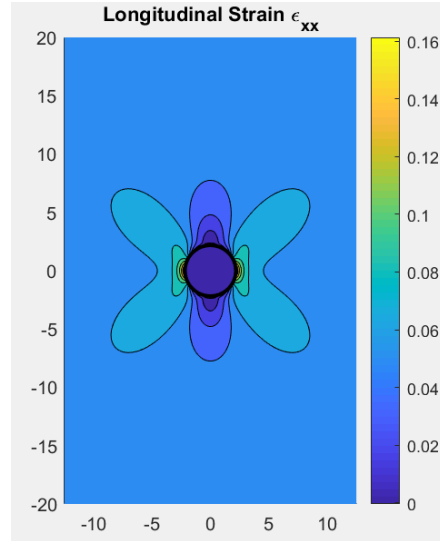


Figure 18: Axial strain at 9% applied strain, with hole.

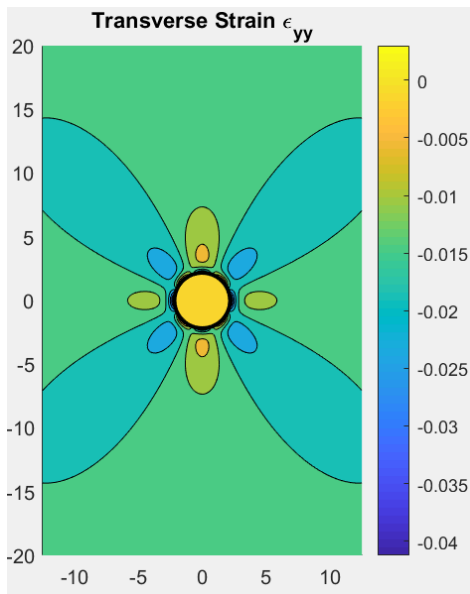


Figure 19: Transverse strain at 3% applied strain, with hole

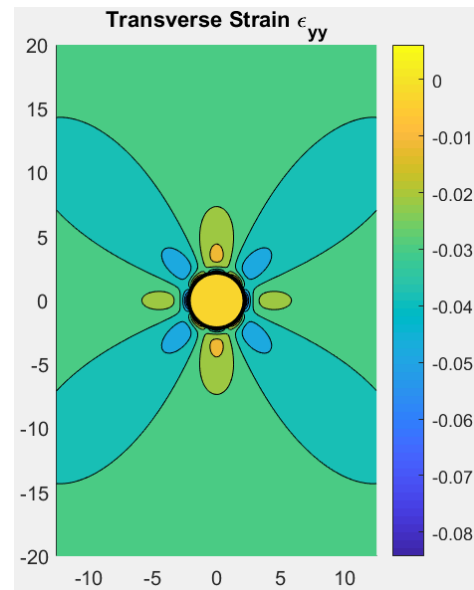


Figure 20: Transverse strain at 9% applied strain, with hole.

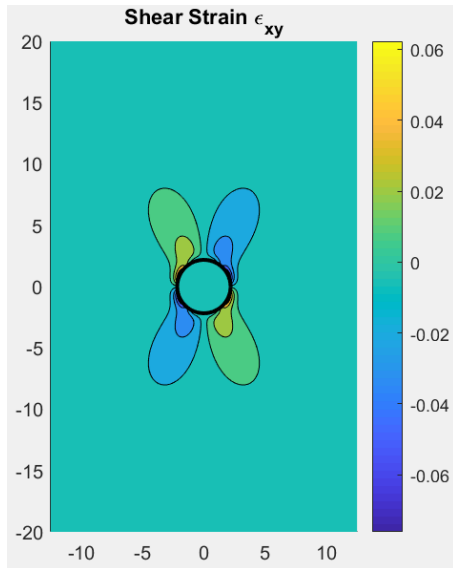


Figure 21: Shear strain at 3% applied strain, with hole

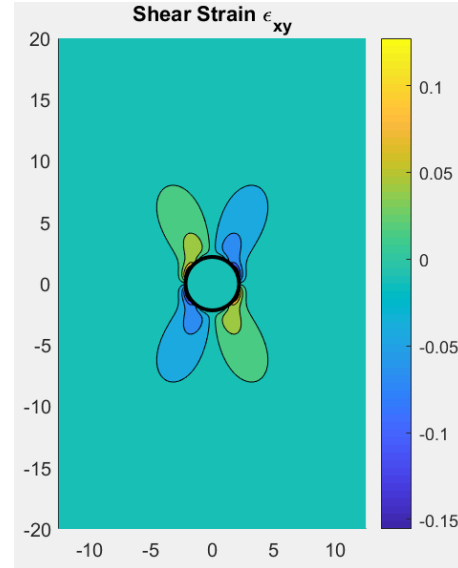


Figure 22: Shear strain at 9% applied strain, with hole.

Discussion

- a. What is the difference in the applied stress-strain response of the specimens with and without a hole? Is this what you would expect?

There is relatively no difference between the applied stress-strain response of the specimens with and without a hole (Figure 4). This is exactly what we expect, because as discussed before in section 3.1, the stress-strain response for a specimen with no hole should be similar to that of the far field stress-strain response for a specimen with a hole, far away from the hole.

- b. Do the strains developed in the specimen without a hole match those predicted by theory? Why or why not? What does this tell you about the noise floor of the measurement technique?

No, they do not match. Our theory predicts that for a uniaxial tension test, the axial strain is uniform throughout the specimen. However, our specimen displayed a strange sinusoidal strain pattern (Figure 5 & 7). Our specimen in particular most likely has some sort of defect or pre-loading applied to it. In general, the strains should not match perfectly because there is inherent error in the DIC technique, which appears as our noise floor. We can calculate our noise floor by

taking the average of the extremes in the color bar for the no hole specimen and taking the difference between that average and the extreme. For example, in Figure 5, we take $\frac{4.35\% + 3.65\%}{2} - (4.35\%) = \pm 0.35\%$. That value is our noise floor, and it differs slightly across different contour plots. The reason this is the noise floor is because in theory, there should be a uniform strain response for a material with no hole, so the range of the strain that appears is the range of error due to the DIC.

- c. Compare the strains developed in the specimens with and without a hole. Do the far field strains match? If not, why might they be different.

The far field strains do not match. For example, if we take a look at Figures 11 & 12, the far field strain far away from the hole at 90 and -90 degrees is -5.8% and -3.3% respectively. The difference is due to the existence of the noise floor, as well as the atypical behavior of the no hole specimen.

- d. For the specimen with a hole, what is the location of the minimum and maximum strains? Does this location match up with where they should be theoretically?

The maximum axial strain occurs at 0 and 180 degrees at the edge of the hole, while the minimum axial strain occurs far from the hole at 90 and -90 degrees (Figure 6 & 8). The maximum transverse strain occurs at the somewhat randomly throughout the specimen, however, this is due to noise, and the maximum transverse strain should occur within the “x” shaped region at the hole (Figure 10 & 12). The theoretical contour plots for the axial strains (Figure 17 & 18) confirm our maximum and minimum axial strain locations for the DIC plots. The 9% strain theoretical contour plot for the transverse strain confirm our maximum strain locations for the DIC plots (Figure 19 & 20), however it does not quite do so for the 3% strain because the “x” shaped pattern has not formed yet. The theoretical contour plots for the transverse strains confirm our minimum strain locations for the DIC plots, however they are located further away from the hole and cover a larger area in the DIC plots.

- e. For the specimen with a hole, what are the values of the maximum and minimum strains in the specimen? What are the predicted values? How much are these values off by (what is the error)? How and why does this error change at higher applied strains?

Table 1: Maximum strains for specimen with hole

Small Strain (3%)				Large Strain (9%)		
	DIC	Theory	Error	DIC	Theory	Error
Axial (%)	6.5	8.418	22.78451	11	17.6	37.5
Trans (%)	-1	-0.4854	106.0157	-1.8	-1.456	23.62637
Shear (%)	0.7	0.7377	5.110479	1.2	15.01	92.00533

Table 2: Minimum strains for specimen with hole

Small Strain (3%)				Large Strain (9%)		
	DIC	Theory	Error	DIC	Theory	Error
Axial (%)	3	0.584	413.6986	5	1.123	345.236
Trans (%)	-2.2	-4.124	46.65373	-3.5	-8.426	58.4619
Shear (%)	-0.5	-0.7311	31.6099	-1	-15.55	93.56913

Upon examination of Table 3 & 4, we can observe that overall, the error increases at higher applied strains. This is because our theoretical model assumes linear elastic conditions and small strains. In addition, our theoretical model is supposed to hold true for a semi-infinite plate, which is not the case in practice. When we stray from those conditions, our error increases as our model becomes less valid.

- f. For the specimen with a hole, do the strains qualitatively match the theoretical strain contour plot? How do they differ? Why might this be the case? Is the error within the noise?

Yes, the DIC strains do qualitatively match the theoretical strain contour plots. Let us inspect the 9% applied strain contour plots because the strain distribution is better developed for the DIC plots at higher strains. For axial strains, figure 8 & 18 both have the maximum strains to the left and right of the hole, and they both have this “butterfly” shaped strain concentration around the hole. For transverse strains, figure 12 & 20 both have an “x” shaped strain concentration around the hole, and they both have maximum strains above and below the hole. For shear strains, figure 16 & 22 both have minimum strains extending from the bottom left to upper right corner around the hole, and maximum strains extending from the bottom right to upper left corner around the

hole. Figure 8 & 18 differ because while in theory the area above and below is at a lower strain than the rest of the specimen, the DIC plot shows that the entire space above and below the hole is at a minimum strain. Figure 12 & 20 differ because for the DIC plot, the region of maximum strain above and below the hole is much larger than that of the theoretical plot. Figure 16 & 22 differ because in theory, the upper left and bottom right region have symmetrical strains, but for the DIC plot, the bottom right region has a greater strain than the upper left. These differences are mainly just due to the noise in the DIC technique. If we take the 9% applied strain for the axial strain plot, our noise floor is $\frac{13.3\% + 11.8\%}{2} - (11.8\%) = \pm 0.75\%$. The error in figure 8 is not within our noise floor, but the error in figure 12 & 16 is within our noise floor.

g. How much error is there between the theoretical strain and the virtual strain gauges?

Does this error get worse at higher applied strains? Why might this be the case?

In order to compare the experimental vs. theoretical strains, virtual strain gauges are utilized for the DIC (Figure 23).

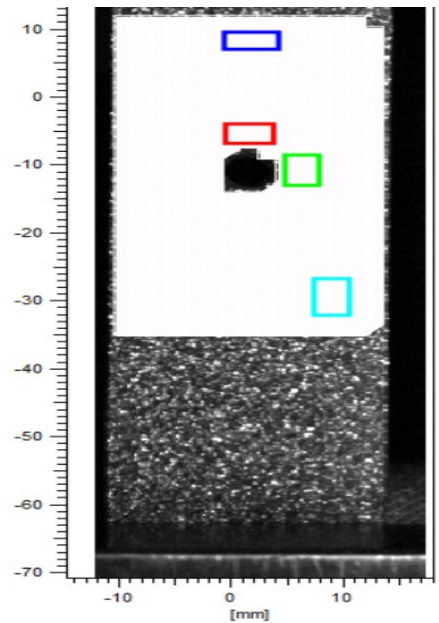


Figure 23: Virtual strain gauge locations

Theoretical strains were obtained from Matlab code. Thus, the following tables were obtained.

Table 3: Experimental vs. Theoretical strain at 3% applied strain, with hole.

Strain Gauge	Small Strain ($\epsilon_{app} = 3\%$)					
	ϵ_{xx}^{SG} (%)	ϵ_{xx}^{Th} (%)	ϵ_{xx}^{Err} (%)	ϵ_{yy}^{SG} (%)	ϵ_{yy}^{Th} (%)	ϵ_{yy}^{Err} (%)
1	2.27111	2.338	2.860992	-0.68294	-0.9383	27.21518
2	2.28107	2.946	22.5706	-0.70496	-1.338	47.31241
3	3.94091	2.362	66.84632	-0.91433	-1.105	17.2552
4	2.55759	2.983	14.26115	-1.01732	-1.501	32.22385

Table 4: Experimental vs. Theoretical strain at 9% applied strain, with hole.

Strain Gauge	Finite Strain ($\epsilon_{app} = 9\%$)					
	ϵ_{xx}^{SG} (%)	ϵ_{xx}^{Th} (%)	ϵ_{xx}^{Err} (%)	ϵ_{yy}^{SG} (%)	ϵ_{yy}^{Th} (%)	ϵ_{yy}^{Err} (%)
1	7.40701	4.751	454.0636	-2.32228	-2.092	11.00765
2	8.26513	5.831	398.1649	-2.41013	-2.772	13.05447
3	11.41372	4.372	161.064	-3.44228	-2.412	42.71476
4	8.51273	5.987	42.1869	-3.14456	-2.913	7.949193

While the errors do not get larger in every single strain gauge at higher applied strains (Table 3 & 4), we can examine the average percent error to see a trend. The average percent error at 3% applied strain is 26.6% and 30.995% for axial and transverse strain, respectively. The average percent error at 9% applied strain is 263.87% and 18.66% for axial and transverse strain, respectively. In theory the higher applied strain should have higher errors because again as mentioned before, our model assumes linear elastic strain and small strain conditions. While we don't see that in the transverse strain, this idea is very apparent when we examine the axial strain average percent error at 9% applied strain.

- h. What are the sources of error present in the experiment? What is the dominant source of error? How could this error be minimized?

Our primary source of error is our theoretical model. When using our model, we assume we have a semi-infinite plate, however that is not the case in reality. In addition, our model is only valid for small strains within the linear elastic strain region. When we exceed 5% applied strain, our model begins to show a higher percent error.

Our secondary source of error is the DIC. The accuracy of DIC heavily depends on the camera resolution that we use, as well as the pixel subset size. In the lab, we lost resolution by having a bigger subset, however that allowed us to better capture overall displacements and strains. We saw in the lab that if the subset size was too large, the DIC camera would not recognize the hole as a hole, which demonstrates the importance and impact that the subset size makes. In addition, the power of the DIC software is a major factor as well, because it is the correlation function that allows us to measure the displacement and strain between subsets.

Our tertiary source of error includes the fact that the specimen twisted out of the plane of the camera. Not only does this slightly alter the strain state of the specimen, but it doesn't allow the camera to be as accurate as it could be if it was normal to the specimen. In addition, our no hole specimen exhibited a very strange DIC contour plot, which made it difficult to compare the strain state of the no hole specimen to that of the holed specimen.

4. Conclusion

In this lab, we utilized digital image correlation to examine the strain state of EPDM rubber specimens with and without a hole under uniaxial tension. What we found was that the theoretical model was more accurate for at smaller applied strains (Tables 1-4). This is evident in the overall larger magnitude of error between the DIC and theoretical strains at a higher applied strain. In addition, we learned qualitatively that the DIC plots matched those of the theoretical plots relatively well, minus a few differences due to noise. Ultimately, digital image correlation is a useful tool for understanding the strain state of a material under a certain load, but it must be noted that the technique is prone to noise, and its precision heavily depends on things such as speckle pattern, subset size, and camera resolution. The theoretical model is a useful tool for predicting the strain state of a holed specimen, but the model will work best under a small applied strain with as close as possible to a semi-infinite plate.

5. References

- [1] McCormick, N. and Lord, J. (2019). *Digital Image Correlation*.

[2] A. Pundle (2019). *ME 354 Laboratory Manual: Digital Image Correlation Formal Lab Report*.

Appendix:

Sample Calculation (at Strain Gauge 1):

Let $r = 7mm$, $a = 2.175mm$, $\sigma_{\infty} = 0.1771MPa$, $E = 6MPa$, $\theta = 90^{\circ}$.

$$\sigma_{rr} = \frac{0.1771(MPa)}{2} \left(\left(1 - \left(\frac{2.175mm}{7mm} \right)^2 \right) + \cos(2 * 90) \left(3 \left(\frac{2.175mm}{7mm} \right)^4 - 4 \left(\frac{2.175mm}{7mm} \right)^2 + 1 \right) \right) = 0.02317 \text{ MPa}$$

$$\sigma_{\theta\theta} = \frac{0.1771(MPa)}{2} \left(\left(1 + \left(\frac{2.175mm}{7mm} \right)^2 \right) - \cos(2 * 90) \left(3 \left(\frac{2.175mm}{7mm} \right)^4 + 1 \right) \right) = 0.186474 \text{ MPa}$$

$$\sigma_{r\theta} = \frac{0.1771(MPa) * \sin(2*90)}{2} \left(3 \left(\frac{2.175mm}{7mm} \right)^4 - 2 \left(\frac{2.175mm}{7mm} \right)^2 - 1 \right) = 0 \text{ MPa}$$

$$\sigma_{xx} = \sigma_{rr} \cos^2(90) + \sigma_{\theta\theta} \sin^2(90) - \sigma_{r\theta} \sin(2*90) = 0.186474 \text{ MPa}$$

$$\sigma_{yy} = \sigma_{rr} \sin^2(90) + \sigma_{\theta\theta} \cos^2(90) - \sigma_{r\theta} \cos(2*90) = 0.02317 \text{ MPa}$$

$$\sigma_{xy} = \sin(90)\cos(90) (0.02317 \text{ MPa} - 0.186474 \text{ MPa}) + 0 = 0 \text{ MPa}$$

$$\epsilon_{xx} = \frac{1}{6 \text{ MPa}} (0.186474 \text{ MPa} - 0.48 * 0.02317 \text{ MPa}) = 0.0292254 \text{ MPa}$$

$$\epsilon_{yy} = \frac{1}{6 \text{ MPa}} (0.02317 \text{ MPa} - 0.48 * 0.186474 \text{ MPa}) = -0.011056 \text{ MPa}$$

$$\gamma_{xy} = \frac{\sigma_{xy}}{G} = 0 \text{ MPa}$$

Excel calculation for Stress vs. Strain Response:

	A	B	C	D	E	F
1	Specimen	With hole				
2	End date	#####				
3	Thickness	2.3 mm		Area (mm ²) =		57.5
4	Width	25 mm				
5	Hole Diam	4.35 mm				
6						
7	Time	Extension	Load	Axial Strain	Stress	
8	(s)	(mm)	(N)	(mm/mm)	(MPa)	
9	0	0	0.87088	0	0.015146	
10	0.1	0.04795	1.16772	0.000366	0.020308	
11	0.2	0.15121	2.11316	0.001154	0.036751	
12	0.3	0.24914	3.08193	0.001902	0.053599	

D10 (Axial strain): =B10/(131) where 131 is the original length of the material

E10 (Stress) =C9/\$F\$3

F3 (Area) = \$B\$3 * \$B\$4

Matlab Code (Theoretical Model):

```
%%%%%%%% Stress and strain for a hole in a plate %%%%%%%%%
```

```
clc; clear; close all
```

```
%% Define sample properties
```

```
E = 6e6; %Young's Modulus
```

```
nu = 0.48; %Poisson's Ratio
```

```
so = 0.361853e6; %Applied stress
```

```
W = 40; %ROI Width
```

```
H = 25; %ROI Height
```

```
a = 2.175; %Hole radius
```

```
G = E/(2*(1+nu));
```

```
%% Set Parameters
```

```
n = 1000; %Spatial Resolution
```

```
x = linspace(-W/2,W/2,n); %x grid
```

```
y = linspace(-H/2,H/2,n); %y grid
```

```
[X,Y] = meshgrid(x,y);
```

```
r = (X.^2 + Y.^2).^0.5; %r grid
```

```
th = atan(Y./X); %theta grid
```

```
xr = a*cos(0:0.01:2*pi); %Hole x
```

```
yr = a*sin(0:0.01:2*pi); %Hole y
```

```
%% Calculate Hoop and Radial Stresses
```

```
srr = so/2.*((1-a^2./r.^2) + (1+3*a^4./r.^4-4*a^2./r.^2).*cos(2.*th));
```

```
srr(r<=a) = 0;
```

```
stt = so/2.*((1+a^2./r.^2) - (1+3*a^4./r.^4).*cos(2.*th));
```

```
stt(r<=a) = 0;
```

```
srt = -so/2.*(1 + 2*a^2./r.^2 - 3*a^4./r.^4).*sin(2.*th);
```

```
srt(r<=a) = 0;
```

```
%% Convert to Cartesian Stress
```

```
sxx = srr.*cos(th).^2 + stt.*sin(th).^2 - srt.*sin(2.*th);
```

```
syy = srr.*sin(th).^2 + stt.*cos(th).^2 + srt.*sin(2.*th);
```

```
sxy = sin(th).*cos(th).*(srr-stt) + srt.*cos(2.*th);
```

```
%% Convert to Strain
```

```
exx = (sxx - nu.*syy)./E;
```

```
eyy = (syy - nu.*sxx)./E;
```

```
exy = sxy/G;
```

```
%% Plot Results
```

```
figure(1)
```

```
hold on
```

```
contourf(Y,X,exx,10)
```

```
plot(xr,yr,'k-','LineWidth',2)
```

```
hold off
```

```
axis equal
```

```
colorbar
```

```
title('Longitudinal Strain \epsilon_x_x')
```

```
figure(2)
hold on
contourf(Y,X,eyy,10)
plot(xr,yr,'k-','LineWidth',2)
hold off
axis equal
colorbar
title('Transverse Strain \epsilon_y_y')
```

```
figure(3)
hold on
contourf(Y,X,exy,10)
plot(xr,yr,'k-','LineWidth',2)
hold off
axis equal
colorbar
title('Shear Strain \epsilon_x_y')
```